


Kramers' degenerate magnetism and superconductivityAdil Amin,^{*} Hao Wu[✉],^{*} Tatsuya Shishidou, and Daniel F. Agterberg[✉]*Department of Physics, University of Wisconsin–Milwaukee, Milwaukee, Wisconsin 53201, USA* (Received 13 July 2023; revised 10 November 2023; accepted 27 November 2023; published 3 January 2024)

Motivated by the recent discovery of odd-parity multipolar antiferromagnetic order in CeRh_2As_2 , we examine the coexistence of such translation invariant Kramers' degenerate magnetic states and superconductivity. We show that the presence of such magnetic states generically suppresses superconductivity, whether it be spin-singlet or spin-triplet, unless the magnetic state drives a symmetry-required pair density wave superconducting order. We apply our results to CeRh_2As_2 , where no pair density wave order appears, and to the loop current order in the cuprates, where such pair density wave superconductivity must appear together with Bogoliubov Fermi surfaces. In the former case, we explain why superconductivity is not suppressed.

DOI: [10.1103/PhysRevB.109.024502](https://doi.org/10.1103/PhysRevB.109.024502)**I. INTRODUCTION**

The discovery of likely field-induced odd-parity superconductivity in CeRh_2As_2 [1] has generated a great deal of interest [2–16]. Subsequent to this, in addition to quadrupolar order [8], CeRh_2As_2 has been found to host odd-parity multipolar antiferromagnetic (AFM) order [17,18]. In particular, nuclear quadrupolar resonance (NQR) and nuclear magnetic resonance (NMR) have observed that this order develops at a temperature below the superconducting transition temperature (T_c). The symmetry of such a state is unusual since it independently breaks parity (\mathcal{P}) and time reversal (\mathcal{T}) symmetries but is invariant under the action of their product \mathcal{PT} . Since \mathcal{PT} is still preserved, electronic states retain the well-known twofold Kramers' degeneracy; hence we shall refer to such magnetic states as Kramers' degenerate magnets. Such order has been referred to as odd parity multipole order [19] and magnetic toroidal order [20,21] in different contexts. Since neither \mathcal{P} nor \mathcal{T} symmetries are present, the electronic dispersion ξ_k does not satisfy the usual relation $\xi_k = \xi_{-k}$. The asymmetry between ξ_k and ξ_{-k} ($\xi_k \neq \xi_{-k}$) naturally opens up the question of what effect Kramers' degenerate magnetic order has on the superconducting state. This question has been addressed previously for multiband systems [19,22] and also for loop current order in cuprates [23–25]. Superconductivity is usually a low energy scale phenomenon; thus it is desirable to develop a general single-band theory to capture the interplay of Kramers' degenerate order and superconductivity. Here we provide such a general theoretical framework that allows us to encompass arbitrary energy dispersions and gap functions, allowing us to draw broad conclusions.

Our theory shows that both spin-singlet and spin-triplet superconductivity are strongly suppressed by such an order (such states can still survive in one-dimensional systems [19]). This theory is exact in the weak-coupling limit. Here T_{c0} is an input parameter. Once T_{c0} is given, changes in the critical

temperature due to Kramers' degenerate magnetic order are quantitatively well described [26]. Our approach is akin to Anderson's theorem which says magnetic order destroys s -wave superconductivity as the Cooper pairs are formed from time-reversal partners. For Kramers' degenerate order considered here both time-reversal symmetry and inversion symmetry are broken and hence there will be a generic suppression of both spin-singlet and spin-triplet superconductivity. However, if the magnetic state belongs to a special symmetry class, then superconductivity can still appear. In particular, if the magnetic state belongs to a vector representation of the point group, then a symmetry-dictated pair density wave (PDW) superconducting state is stabilized. Furthermore, we find this magnetic order often implies the existence of Fermi surfaces in the superconducting states. Such Fermi surfaces are called Bogoliubov Fermi surfaces (BFSs). When the magnetic state leads to symmetry-required PDW superconductivity, we find that the PDW order reduces the size of the Bogoliubov Fermi surfaces, providing a natural microscopic mechanism for the appearance of such PDW order. We apply this framework to superconductivity coexisting with odd-parity multipolar AFM order in CeRh_2As_2 and coexisting with the loop current order in the cuprates. In a recent paper we also apply the general framework developed here to obtain a nematic BFSs in the tetragonal phase of $\text{FeSe}_{1-x}\text{S}_x$ [21]. Such BFSs have recently been observed in ARPES measurements for $\text{FeSe}_{1-x}\text{S}_x$ [27].

II. ODD PARITY ENERGY DISPERSION

As discussed above, Kramers' degenerate magnetic order gives rise to asymmetry between the electronic dispersions ξ_k and ξ_{-k} . This asymmetry is the key ingredient in our theory and we define $\xi_{-,k} = (\xi_k - \xi_{-k})/2$ to quantify this. The \mathbf{k} dependence of $\xi_{-,k}$ is governed by the symmetry of Kramers' degenerate magnetic order [20]. Since these magnetic orders are translation invariant, they correspond to odd-parity irreducible representations of the crystallographic point group. Therefore, $\xi_{-,k}$ can be constructed by forming products of momentum components k_i that belong to the corresponding

*These authors contributed equally to this work.

irreducible representation of the crystallographic point group. Some examples of the predicted form of $\xi_{-,k}$ can be found in [19,22,28–34] and the recent experimental observation of this has been reported in Mn_2Au [28]. Here we discuss what form $\xi_{-,k}$ takes for the observed odd-parity AFM order in CeRh_2As_2 and for the loop current order in the cuprates.

In CeRh_2As_2 , with space group $P4/nmm$, there are two Ce atoms per unit cell. Including a single Kramers' doublet on each Ce site leads to the tight-binding Hamiltonian [1],

$$\begin{aligned} H_0 &= \epsilon_{00,k} \tau_0 \sigma_0 + \epsilon_{x0,k} \tau_x \sigma_0 + \epsilon_{y0,k} \tau_y \sigma_0 \\ &\quad + \epsilon_{zx,k} \tau_z \sigma_x + \epsilon_{zy,k} \tau_z \sigma_y + \epsilon_{zz,k} \tau_z \sigma_z \\ &= [t_1 (\cos k_x + \cos k_y) - \mu] \tau_0 \sigma_0 + t_{c,1} \cos \frac{k_z}{2} \cos \frac{k_x}{2} \\ &\quad \times \cos \frac{k_y}{2} \tau_x \sigma_0 + t_{c,2} \sin \frac{k_z}{2} \cos \frac{k_x}{2} \cos \frac{k_y}{2} \tau_y \sigma_0 \\ &\quad + \alpha_R (\sin k_y \tau_z \sigma_x - \sin k_x \tau_z \sigma_y) \\ &\quad + \lambda \sin k_z (\cos k_x - \cos k_y) \sin k_x \sin k_y \tau_z \sigma_z. \end{aligned} \quad (1)$$

The τ_i Pauli matrices encode the Ce site basis and the σ_i Pauli matrices encode the spin basis. Here α_R and λ are the Rashba and Ising spin-orbit couplings. This has the following energy dispersion:

$$\xi_{1,2,k} = \epsilon_{00,k} \pm \sqrt{\epsilon_{x0,k}^2 + \epsilon_{y0,k}^2 + \epsilon_{zx,k}^2 + \epsilon_{zy,k}^2 + \epsilon_{zz,k}^2}. \quad (2)$$

This Hamiltonian gives rise to two bands where 1,2 refers to the + and – bands, respectively, each of which has a pseudospin degeneracy with the property that $\xi_{1,2,k} = \xi_{1,2,-k}$.

To Eq. (1), we add the minimal coupling to the odd-parity AFM order. This order is of opposite sign on the two Ce sites in the unit cell and the Ce moments are oriented along the z axis [17,18]. Consequently, we write this coupling as $H_c = M_z \tau_z \sigma_z$. The resulting Hamiltonian gives rise to two doubly degenerate (the twofold degeneracy is a pseudospin degeneracy) bands. Treating H_c as a perturbation to H_0 yields

$$\xi_{-,k} = \pm \frac{M_z \lambda \sin k_z (\cos k_x - \cos k_y) \sin k_x \sin k_y}{\sqrt{\epsilon_{x0,k}^2 + \epsilon_{y0,k}^2 + \epsilon_{zx,k}^2 + \epsilon_{zy,k}^2 + \epsilon_{zz,k}^2}} \tilde{\sigma}_0, \quad (3)$$

where $\tilde{\sigma}_0$ denotes the pseudospin degeneracy and the \pm denotes that $\xi_{-,k}$ has a different sign on the two bands $\xi_{1,2,k}$. A key feature of the $\xi_{-,k}$ is that even though it has the same form for both pseudospin partners, it is generated through the spin-orbit coupling term λ . Formally, $\xi_{-,k}$ has a momentum structure that belongs to the A_{1u} representation of the D_{4h} point group. We illustrate the momentum asymmetry of $\xi_{-,k}$ by plotting the change to $\xi_{1,2,k}$ due to the presence of Kramers' degenerate order in Fig. 1 for momenta near the Brillouin zone boundary.

The form of $\xi_{-,k}$ for loop current order in the cuprates has been derived earlier and takes the form [23,35–38]

$$\xi_{-,k} = 2J [\sin k_x - \sin k_y - \sin(k_x - k_y)] \sigma_0, \quad (4)$$

where J is the strength of the order. Physically, this term originates from orbital currents that form closed loops within the CuO_2 unit cell. In this case, unlike for CeRh_2As_2 above, spin-orbit coupling does not play a role in the origin of $\xi_{-,k}$. Formally, for the loop current order, the momentum structure

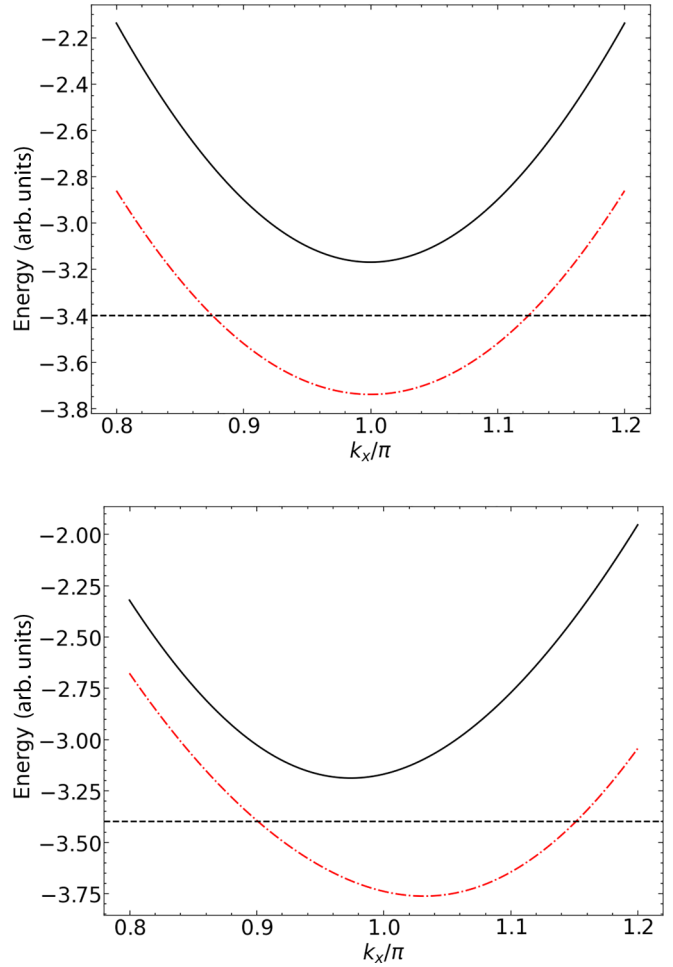


FIG. 1. Band dispersions for CeRh_2As_2 . *Top*: energy dispersion for CeRh_2As_2 with $k_y = \frac{0.4\pi}{a}$, $k_z = \frac{0.4\pi}{a}$, $t_1 = 5$, $t_{c1} = 0.1$, $t_{c2} = 0.1$, $\alpha_R = 0.3$, $\lambda = 0.3$ and with $a = 1$ and $\mu = -3.4$. Note that the dispersion is symmetric about $k_x = \pi$. The black band corresponds to $\xi_{1,k}$, while the red band corresponds to $\xi_{2,k}$. *Bottom*: energy dispersion for CeRh_2As_2 after the addition of Kramers' degenerate order with $M_z = 0.5$. Notice the asymmetry of the dispersion around $k_x = \pi$.

of $\xi_{-,k}$ belongs to the E_u representation of the D_{4h} point group. In contrast to the odd-parity multipole AFM order in CeRh_2As_2 , here the momentum structure of $\xi_{-,k}$ belongs to a vector representation of the D_{4h} point group. This, as we shall see later, leads to the stabilization of PDW superconductivity for the cuprates.

III. GENERAL THEORY

The Kramers' degeneracy that is retained with the presence of Kramers' degenerate magnetic order allows a single band theory for superconductivity [39,40]. In the weak coupling limit, this can be formulated for arbitrary Fermi surfaces, gap functions, and $\xi_{-,k}$ and this further will allow this physics to be treated within the framework of quasiclassical theory, a powerful framework within which to examine superconductivity [26]. We consider the following single-band

Hamiltonian:

$$H = \sum_{ks} \varepsilon_k c_{ks}^\dagger c_{ks} + \frac{1}{2} \sum_{kk'\alpha\beta\alpha'\beta'} V_{\alpha\beta\alpha'\beta'}(\mathbf{k}, \mathbf{k}') \times c_{k+\frac{q}{2},\alpha}^\dagger c_{-k+\frac{q}{2},\beta}^\dagger c_{-k'+\frac{q}{2},\beta'} c_{k'+\frac{q}{2},\alpha'}, \quad (5)$$

where the operator c_{ks}^\dagger (c_{ks}) creates (annihilates) electrons with momentum \mathbf{k} and spin s ; $s, \alpha, \beta, \alpha', \beta' = \uparrow, \downarrow$; \mathbf{q} is the center-of-mass momentum of the Cooper pairs; $\varepsilon_k \equiv \xi_k - \mu = \xi_{+,k} + \xi_{-,k} - \mu$, where $\xi_{+,k} = (\xi_k + \xi_{-k})/2$ is the usual \mathbf{k} symmetric dispersion included for single-band theories and μ is the chemical potential. The role of Kramers' degenerate magnetic order is included through the addition of $\xi_{-,k}$. Here we explicitly include the Cooper pair center of mass momentum since later we find that symmetry requires this must be nonzero for Kramers' degenerate magnetic order belonging to a vector representation of the point group.

Prior to presenting the results of our analysis, we note that generally Kramers' degenerate magnetic order leads to mixing between even parity, pseudospin-singlet and odd parity, pseudospin-triplet superconductivity. This can be understood from the Ginzburg-Landau (GL) theory. In particular, consider an even parity order parameter ψ , an odd parity order parameter η , and a Kramers' degenerate magnetic order parameter M . Then symmetry allows the following term $iM(\psi\eta^* - \eta\psi^*)$ in the GL free energy, which ensures a singlet-triplet mixed order parameter of the form $\psi + i\eta$. However, in the single band limit we consider here, it is possible to show that this pseudospin singlet-triplet mixing vanishes if we assume that the pairing interactions are not changed by Kramers' degenerate magnetic order. This is justified if $\xi_{-,k}$ has a much smaller energy scale than the electronic bandwidth, which we assume here. Hence we consider each pairing channel independently. For pseudospin singlet order, we take $V_{\alpha\beta\alpha'\beta'}(\mathbf{k}, \mathbf{k}') = \frac{V_s}{2} [f_k i \sigma_2]_{\alpha\beta} [f_{k'} i \sigma_2]_{\alpha'\beta'}$, while for pseudospin triplet order we take $V_{\alpha\beta\alpha'\beta'}(\mathbf{k}, \mathbf{k}') = -\frac{V_s}{2} [\mathbf{d}_k \cdot \boldsymbol{\sigma} i \sigma_2]_{\alpha\beta} [\mathbf{d}_{k'} \cdot \boldsymbol{\sigma} i \sigma_2]_{\alpha'\beta'}$ and assume that both f_k and \mathbf{d}_k can be chosen real—in practice this applies to singly degenerate superconducting irreducible representations. It is not difficult to generalize this to higher-dimensional irreducible representations.

Since we consider finite momentum pairing with wavevector \mathbf{q} , the mean-field limit of superconductivity is described by the following Bogliubov-de Gennes Hamiltonian:

$$\mathcal{H}_{BDG} = \begin{pmatrix} \xi_{+,k+\frac{q}{2}} + \xi_{-,k+\frac{q}{2}} - \mu & \Delta_{k,q} \\ -\Delta_{k,q}^* & -\xi_{+,-k+\frac{q}{2}} - \xi_{-,-k+\frac{q}{2}} + \mu \end{pmatrix}. \quad (6)$$

This leads to the following free energy:

$$\Omega_s - \Omega_n = \left\{ -2k_B T \sum_k \ln \left[\cosh \left(\frac{\beta E_{k,q}}{2} \right) \right] + \frac{|\Delta_q|^2}{V_s} \right\} - \left\{ -2k_B T \sum_k \ln \left[\cosh \left(\frac{\beta E_{k,q,0}}{2} \right) \right] \right\}, \quad (7)$$

where $E_{k,q} \equiv (\Delta\varepsilon)_{k,q} + \sqrt{\varepsilon_{k,q}^2 + |\Delta_q f_k|^2}$ with $(\Delta\varepsilon)_{k,q} \equiv \frac{1}{2}(\varepsilon_{k+\frac{q}{2}} - \varepsilon_{-k+\frac{q}{2}})$ and $\varepsilon_{k,q} \equiv \frac{1}{2}(\varepsilon_{k+\frac{q}{2}} + \varepsilon_{-k+\frac{q}{2}})$, $E_{k,q,0} \equiv (\Delta\varepsilon)_{k,q} + \sqrt{\varepsilon_{k,q}^2}$, and V_s is the pairing interaction. Equation (7)

applies to pseudospin-singlet order; for the pseudospin-triplet order, $|f_k|^2$ is replaced by $|\mathbf{d}_k|^2$. Minimizing this free energy with respect to $|\Delta_q|$ and \mathbf{q} leads to the gap equation and the condition on \mathbf{q} that ensures a vanishing supercurrent

$$\ln \left(\frac{T}{T_{c0}} \right) = \left\langle 2\pi k_B T |f_k|^2 \operatorname{Re} \sum_{n=0}^{\infty} \left(\frac{1}{\delta} - \frac{1}{\hbar\omega_n} \right) \right\rangle_k, \quad (8)$$

$$\left\langle \frac{\partial(\Delta\varepsilon)_{k,q}}{\partial \mathbf{q}} |f_k|^2 \operatorname{Im} \sum_{n=0}^{\infty} \frac{1}{\delta(\delta + \hbar\omega_n + i(\Delta\varepsilon)_{k,q})} \right\rangle_k = 0, \quad (9)$$

where $\delta \equiv \sqrt{(\hbar\omega_n + i(\Delta\varepsilon)_{k,q})^2 + |\Delta_q|^2 |f_k|^2}$ and ω_n is the Matsubara frequency which satisfies $\hbar\omega_n = (2n+1)\pi k_B T$, $n \in \mathbb{Z}$. Throughout this work, we adopt the convention that the average over the Fermi surface $\langle |f_k|^2 \rangle_k = 1$. This average over the Fermi surface is weighted by the momentum-dependent density of states. By numerically solving this set of equations, we can find the gap and the optimal \mathbf{q} as functions of T . As shown in the Appendix, the Green's function and the anomalous Green's function are

$$\hat{G} = -\frac{\hbar(\varepsilon_{-k+\frac{q}{2}} + i\hbar\omega_n)\sigma_0}{(\varepsilon_{-k+\frac{q}{2}} + i\hbar\omega_n)(\varepsilon_{k+\frac{q}{2}} - i\hbar\omega_n) + |\psi(\mathbf{k}, \mathbf{q})|^2}, \quad (10)$$

$$\hat{F} = \frac{\hbar\hat{\Delta}}{(\varepsilon_{-k+\frac{q}{2}} - i\hbar\omega_n)(\varepsilon_{k+\frac{q}{2}} + i\hbar\omega_n) + |\psi(\mathbf{k}, \mathbf{q})|^2}, \quad (11)$$

where σ_0 is the identity matrix and $\hat{\Delta}$ is the gap matrix. As can be also seen in the Appendix, for the pseudospin triplet $|\psi(\mathbf{k}, \mathbf{q})|^2$ is replaced by $|\mathbf{d}(\mathbf{k}, \mathbf{q})|^2$.

To gain an understanding of the role of Kramers' degenerate magnetic order, we initially consider T near T_c . The equation determining the critical temperature T_c^q is

$$\ln \left(\frac{T_c^q}{T_{c0}} \right) = \left\langle |f_k|^2 \left\{ \psi \left(\frac{1}{2} \right) - \operatorname{Re} \left[\psi \left(\frac{1}{2} + \frac{i(\Delta\varepsilon)_{k,q}}{2\pi k_B T_c^q} \right) \right] \right\} \right\rangle_k, \quad (12)$$

where T_{c0} is the critical temperature for $(\Delta\varepsilon)_{k,q} = 0$, the digamma function $\psi(z) = -\gamma + \sum_{n=0}^{\infty} \left(\frac{1}{n+1} - \frac{1}{n+z} \right)$, and γ is the Euler-Mascheroni constant. Assuming $|\mathbf{q}| \ll |\mathbf{k}|$, we have $(\Delta\varepsilon)_{k,q} = \xi_{-,k} + \frac{q}{2} \cdot \nabla \xi_{+,k}$. The expression $\psi(\frac{1}{2}) - \operatorname{Re}[\psi(\frac{1}{2} + \frac{i(\Delta\varepsilon)_{k,q}}{2\pi k_B T_c^q})]$ is intrinsically negative, which yields $T_c^q < T_{c0}$. From the monotonic decreasing dependence of the digamma function, we find that T_c^q is decreasing with increasing $|(\Delta\varepsilon)_{k,q}|$. Eventually, T_c^q will become zero, i.e., superconductivity is destroyed. Using the asymptotic expansion of the digamma function, the critical value for $|(\Delta\varepsilon)_{k,q}|$ corresponding to $T_c = 0$ is given by

$$\left\langle |f_k|^2 \ln \left(\frac{|(\Delta\varepsilon)_{k,q}|}{2\pi k_B T_{c0}} \right) \right\rangle_k = \psi \left(\frac{1}{2} \right). \quad (13)$$

We conclude that once the magnitude of $(\Delta\varepsilon)_{k,q}$ becomes on the order of $k_B T_{c0}$ superconductivity is destroyed. We note that the usual Pauli limiting field, H_P , for an s -wave superconductor is given by $\mu_B H_P = \Delta_0/\sqrt{2}$; hence, throughout this paper, we choose to express $(\Delta\varepsilon)_{k,q}$ in units of $\mu_B H_P$ to provide some context. Importantly, since $(\Delta\varepsilon)_{k,q}$ depends not only on $\xi_{-,k}$, but also on \mathbf{q} , it is possible that $(\Delta\varepsilon)_{k,q}$ can become small even if $\xi_{-,k}$ is larger than the superconducting gap. To

illustrate this, it is useful to consider an example with $\xi_{+,k} = \frac{\hbar^2 k^2}{2m}$ and $\xi_{-,k} = \alpha k_x$. Then, $(\Delta\varepsilon)_{k,q} = \alpha k_x + \frac{\hbar^2}{2m}(q_x k_x + q_y k_y)$. The choice $\mathbf{q} = (q_x, q_y) = (-\frac{2m\alpha}{\hbar^2}, 0)$ will cancel the $\xi_{-,k}$ term making $(\Delta\varepsilon)_{k,q} = 0$. Therefore, the critical temperature remains unchanged from T_{c0} in spite of a $\xi_{-,k}$ that can be much larger than the gap.

To understand in more detail how a PDW state with a nonzero \mathbf{q} can resurrect a suppressed T_c due to $\xi_{-,k}$, we carry out a small $(\Delta\varepsilon)_{k,q}$ expansion. The critical temperature is then determined by

$$\ln\left(\frac{T_c^q}{T_{c0}}\right) = \frac{7\zeta(3)}{(2\pi k_B T_c^q)^2} \times \left\langle |f_k|^2 \left[-\xi_{-,k}^2 - \frac{\hbar^2(\mathbf{q} \cdot \mathbf{v})^2}{4} - \hbar \xi_{-,k} \mathbf{q} \cdot \mathbf{v} \right] \right\rangle_k,$$

where $\mathbf{v}(\mathbf{k}) \equiv \frac{1}{\hbar} \nabla \xi_{+,k}$ is the velocity. Only the third term $(-\hbar \xi_{-,k} \mathbf{q} \cdot \mathbf{v})$ can be positive and hence increase T_c^q . Thus the existence of a PDW state depends on a nonzero average $\langle |f_k|^2 [-\hbar \xi_{-,k} \mathbf{q} \cdot \mathbf{v}] \rangle_k$. Since the components of the velocity \mathbf{v} belong to a vector representation of the point group, the only way to get this average nonzero is to require that the momentum structure of $\xi_{-,k}$ also belongs to a vector representation. This implies that Kramers' degenerate magnetic order belongs to a vector representation of the point group. Indeed, when Kramers' degenerate magnetic order belongs to a vector representation, symmetry implies that the Ginzburg-Landau free energy contains a nonvanishing Lifshitz invariant of the form $\sum_j \gamma_j [\psi(D_j \psi)^* + \psi^*(D_j \psi)]$ with $D_j \equiv -i\nabla_j - 2eA_j$, which guarantees the appearance of a PDW state with nonzero \mathbf{q} . This symmetry-dictated PDW order typically takes the form $\psi = \psi_0 e^{i\mathbf{q} \cdot \mathbf{r}}$ with a single-plane wave, unlike the multiple plane-wave solutions often associated with PDW order [41]. The existence of Lifshitz invariants, and the concomitant finite momentum PDW pairing, is important for the superconducting diode effect [42–45]. This suggests that superconductivity coexisting with Kramers' degenerate magnetic order provides a route toward creating the superconducting diode effect.

In addition to generating PDW states, Kramers' degenerate magnetic order can also lead to novel low-energy excitation spectra. In particular, by finding the poles of the Green's function G , we can obtain the quasiparticle dispersion

$$E = (\Delta\varepsilon)_{k,q} \pm \sqrt{\epsilon_{k,q}^2 + |\Delta_q f_k|^2}. \quad (14)$$

In principle, because of the appearance of $(\Delta\varepsilon)_{k,q}$ in this expression, Bogoliubov Fermi surfaces (BFSs) can exist. These BFSs are given by $E = 0$ and appear for \mathbf{k} where $(\Delta\varepsilon)_{k,q}$ is larger than $|\Delta_q f_k|$. Indeed, these are guaranteed to appear when there are gap nodes present, i.e., $f_k = 0$ (or $|\mathbf{d}_k| = 0$) provided that $(\Delta\varepsilon)_{k,q}$ does not also vanish on these nodes. When this occurs, $(\Delta\varepsilon)_{k,q}$ inflates the nodes of the original gap functions into Bogoliubov Fermi surfaces [46–49]. In a recent paper [21] we carry out a detailed analysis of the existence of Bogoliubov Fermi surfaces in $\text{FeSe}_{1-x}\text{S}_x$.

IV. APPLICATION TO CeRh_2As_2

In addition to Eq. (3) for $\xi_{-,k}$, we require a description of the normal state to apply our results to CeRh_2As_2 . DFT results

[7,50] yield a Fermi surface as depicted in Fig. 2. They further reveal that the majority of the density of states (DOS) ($\sim 80\%$) is concentrated on the Fermi surface structures near the X–M line, which we refer to as beans. Here we include only those beans and, for simplicity, ignore the c -axis dependence of $\xi_{+,k}$ (this assumption does not qualitatively change our results). Furthermore, we assume that a $d_{x^2-y^2}$ gap structure as depicted in Fig. 2 appears when no magnetic field is applied. This assumption also does not qualitatively change the results unless the gap function has nodes on the beans. We briefly comment on this possibility later. To describe these beans, we develop a power series expansion in powers of $\delta k_x, \delta k_y$ centered about the minima of the band along the X–M line. Explicitly considering a bean centered at $(\tilde{k}_x, \tilde{k}_y) = (\frac{\pi}{a}, \frac{0.4\pi}{a})$, we have the dispersion

$$\xi_{+,k} = \alpha(\delta k_x)^2 + \beta(\delta k_y)^2 + \gamma_1(\delta k_x)^2(\delta k_y) + \gamma_2(\delta k_y)^3. \quad (15)$$

Mirror symmetry prevents terms odd in δk_x appearing in this expression. We also expand $\xi_{-,k}$ in Eq. (3) around the centers of the beans. For the pocket centered at $(\tilde{k}_x, \tilde{k}_y)$, we take $\xi_{-,k} = \tilde{\lambda} \delta k_x a \sin k_z$, where

$$\tilde{\lambda} = \frac{-M_z \lambda [1 + \cos(\tilde{k}_y)]}{\alpha_R}. \quad (16)$$

The numerical solution of the linearized gap equation is shown in Fig. 3. Because Kramers' degenerate magnetic order does not belong to a vector representation, a PDW state is not required by symmetry in this case. Thus, when $\xi_{-,k}$ becomes sufficiently large, superconductivity is suppressed as seen in Fig. 3. However, this is not observed in experiment [17,18], i.e., there is no change seen to superconductivity upon entering the magnetic state, which raises the following question: how does superconductivity still survive? Here we suggest that the explanation for this persistence hinges on the value of $\tilde{\lambda}$ defined in Eq. (16). This depends strongly on the ratio of the Ising coupling (λ) to the Rashba spin-orbit coupling (α_R). An upper bound to this ratio, and hence $\tilde{\lambda}$, can be estimated

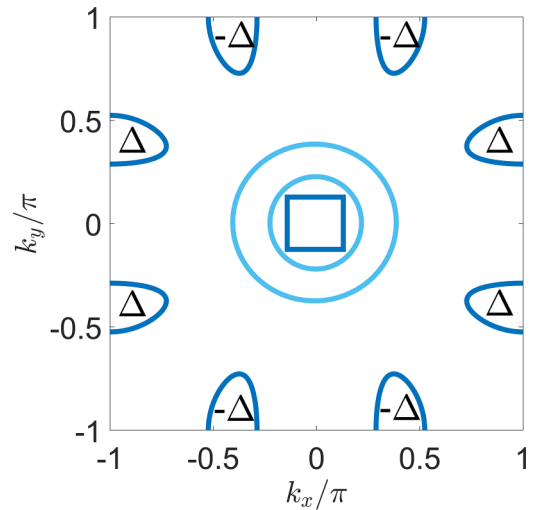


FIG. 2. Sketch of the normal state Fermi surface of CeRh_2As_2 for $k_z = 0$ found from renormalized DFT calculations. The majority of the density of states sits on the beans. The $d_{x^2-y^2}$ pairing symmetry considered here is denoted by the Δ values as shown.

using density functional theory (DFT) calculations [51]. In particular, for Kramers' degenerate bands, the band splitting by a Zeeman field can be quantified by calculating effective \tilde{g} factors. These \tilde{g} factors have been calculated by DFT and quantify the energy splitting between Kramers' doublets for fields applied along the x , y , and z directions. Comparing the DFT results to the effective g factors calculated from Eq. (1)

$$\frac{\tilde{g}_{\mathbf{k},z}^2}{\tilde{g}_{\mathbf{k},x}^2 + \tilde{g}_{\mathbf{k},y}^2} \approx \frac{(\delta k_x)^2 \{ \cos^2(\tilde{k}_y/2) [t_{c,1}^2 \cos^2(k_z/2) + t_{c,2}^2 \sin^2(k_z/2)] + \sin^2(\tilde{k}_y) \alpha_R^2 \tilde{\lambda}^2 / M_z^2 \}}{\alpha_R^2 \sin^2(\tilde{k}_y)} > \tilde{\lambda}^2 / M_z^2. \quad (17)$$

We further estimate $M_z \approx \mu_B H_P$, where H_P is the usual Pauli limiting field since the temperature scale for M_z is of the order of the critical temperature of superconductivity. From DFT it is found that, after averaging over the Fermi surface of the beans, $\sqrt{g_{\mathbf{k},z}^2 / (g_{\mathbf{k},x}^2 + g_{\mathbf{k},y}^2)} \approx 0.2$ [51], and hence $\frac{ak_F \tilde{\lambda}}{\mu_B H_P} < 0.1$ (where we have used that $ak_F \approx 0.5$). The ratio of ak_F is determined by the size of the beans to the size of the Brillouin zone. The condition $\frac{ak_F \tilde{\lambda}}{\mu_B H_P} < 0.1$ is shown as the shaded region in Fig. 3. We note that the actual value of $\tilde{\lambda}$ is likely much smaller due to the use of the final inequality in Eq. (17). Thus superconductivity persists despite the presence of Kramers' degenerate magnetic order. Recent ARPES measurements [53,54] have found quasi-two-dimensional (2D) Fermi surfaces with a large density of states near the zone boundary consistent with the beans considered in this manuscript. While the detailed structure of the Fermi surfaces obtained the ARPES measurements may be different than that considered here, nevertheless the arguments outlined above giving rise to a small $\tilde{\lambda}$ will still stand and superconductivity will still persist.

While the pairing state we consider above has $d_{x^2-y^2}$ symmetry, it is nodeless on the Fermi surface beans which do not

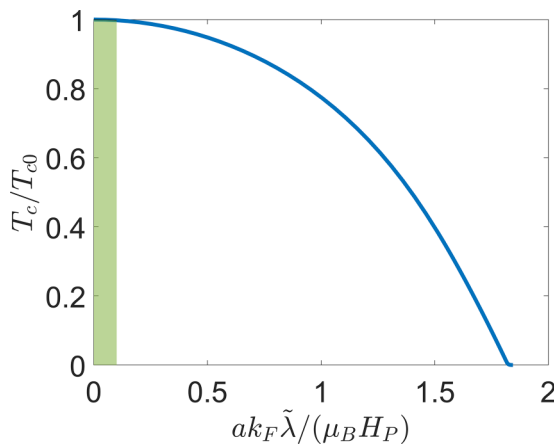


FIG. 3. Transition temperature as a function of the antisymmetric coupling parameter λ in CeRh₂As₂. The parameter a is the lattice constant; $k_F \equiv \sqrt{\frac{\mu}{\alpha\beta}}$ is the natural unit for δk_x and δk_y . We choose the values $\alpha = \frac{1}{(1.25)^2}$, $\beta = \frac{1}{(0.55)^2}$, $\mu = 0.7$, and $\gamma_1 = 0.75$, $\gamma_2 = -0.9$. The Pauli limiting field energy scale $\mu_B H_P = \Delta_0 / \sqrt{2}$, where $\Delta_0 = 1.764 k_B T_{c0}$. The shaded region describes the estimated allowed parameter regime for CeRh₂As₂.

reveals that $\xi_{-\mathbf{k}}$ generated by Kramers' degenerate magnetic order is too small to suppress superconductivity. More specifically, the effective \tilde{g} factor for a particular field orientation \mathbf{h} and momentum \mathbf{k} is given by [52] $\tilde{g}_{\mathbf{k},\mathbf{h}}^2 = \frac{\epsilon_{x0,\mathbf{k}}^2 + \epsilon_{y0,\mathbf{k}}^2 + (\epsilon_{3,\mathbf{k}} \cdot \hat{\mathbf{h}})^2}{\epsilon_{x0,\mathbf{k}}^2 + \epsilon_{y0,\mathbf{k}}^2 + \epsilon_{3,\mathbf{k}}^2}$, where $\epsilon_{3,\mathbf{k}} = (\epsilon_{zx,\mathbf{k}}, \epsilon_{zy,\mathbf{k}}, \epsilon_{zz,\mathbf{k}})$. The ratio of relevance for $\tilde{\lambda}$ is $\frac{\tilde{g}_{\mathbf{k},z}^2}{\tilde{g}_{\mathbf{k},x}^2 + \tilde{g}_{\mathbf{k},y}^2}$. Near the beans, this ratio is

intersect the $d_{x^2-y^2}$ nodes. However, the $d_{x^2-y^2}$ gap will have nodes along the Γ -centered Fermi surfaces, possibly allowing for Bogoliubov Fermi surfaces to appear in the superconducting state. However, these nodes will not be inflated to Bogoliubov Fermi surfaces since $(\Delta\epsilon)_k$ vanishes on the nodes of the $d_{x^2-y^2}$ gap. We can further consider other gap functions with nodes to see if Bogoliubov Fermi surfaces are expected. For example, nodes can appear on the beans for a d_{xy} -like gap. The beans will then have nodes where they intersect the Brillouin zone face. However, these nodes will also not be inflated to form Bogoliubov Fermi surfaces because again $(\Delta\epsilon)_k$ vanishes on these nodes. Consequently, we do not expect Bogoliubov Fermi surfaces to appear as a consequence of Kramers' degenerate magnetic order in CeRh₂As₂ for any pairing symmetry.

V. APPLICATION TO LOOP CURRENT ORDER IN CUPRATES

The normal state is given by the dispersion $\xi_{+,k} = -2t(\cos k_x + \cos k_y) - 4t' \cos(k_x) \cos(k_y)$, where t and t' are the nearest and next nearest neighbor hoppings on the square

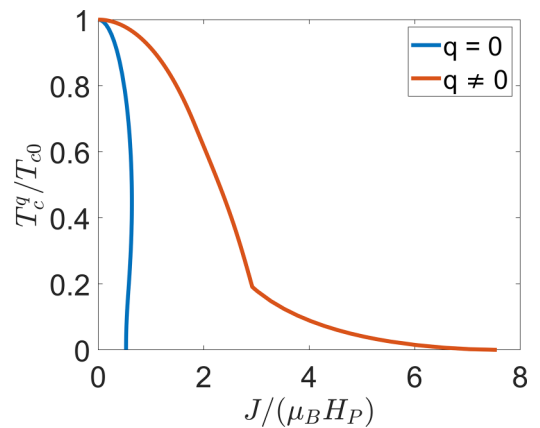


FIG. 4. Transition temperature as a function of the loop current order parameter for both $\mathbf{q} = 0$ and finite \mathbf{q} theories. The Pauli limiting field energy scale $\mu_B H_P = \Delta_0 / \sqrt{2}$, where $\Delta_0 = 1.764 k_B T_{c0}$. Using hopping parameter t as the energy scale, we choose $t' = -0.25$, $\mu = -0.9$. We can observe a nonmonotonic behavior in the $\mathbf{q} = 0$ plot. This kind of behavior typically suggests the existence of a PDW state. This reveals that PDW order is energetically favorable since it shrinks the size of the Bogoliubov Fermi surfaces.

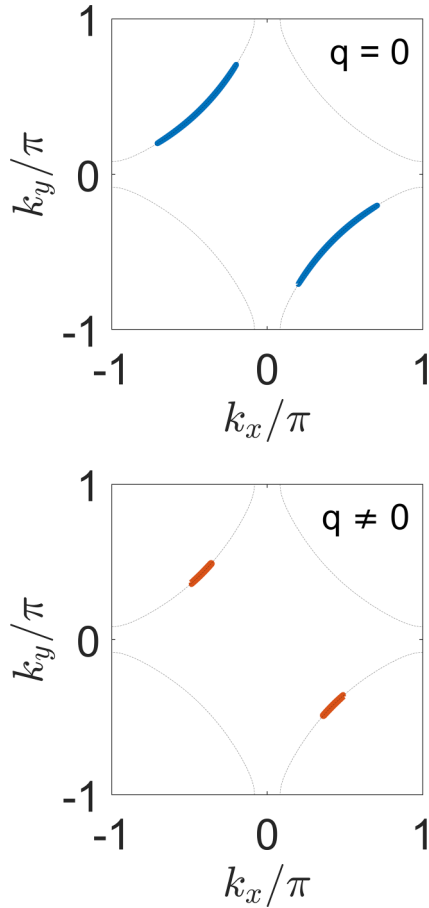


FIG. 5. Bogoliubov Fermi surfaces. The upper plot is for $q = 0$; the lower plot is for $q \neq 0$.

2D lattice [23]. Equation (4) above gives $\xi_{-\mathbf{k}}$. The gap function is taken to be $\Delta_{\mathbf{k},\mathbf{q}} = \Delta_{\mathbf{q}} f_{\mathbf{k}} = \Delta_{\mathbf{q}} C (\cos k_x - \cos k_y)$ with normalization factor C (determined by $\langle |f_{\mathbf{k}}|^2 \rangle_{\mathbf{k}} = 1$). Since Kramers' degenerate magnetic order belongs to a vector representation, our general results imply that a PDW state is stabilized by the loop current order. In Fig. 4, we compare the calculated values for T_c with and without the PDW order. Remarkably, the maximum J value for the PDW state is about 15 times larger than the $\mathbf{q} = 0$ state. In addition, since the d -wave gap has nodes, the loop current order will give rise to BFSs. As shown in Fig. 5, we find that the BFSs are strongly shrunk due to the PDW order. The gain in condensation energy due to the shrinking of the BFSs provides an energetic mechanism to stabilize the PDW state. The properties of such BFSs have been examined previously in the cuprates when there is no PDW order [23,25,55]. There it has been discussed that specific heat measurements will reveal a residual Sommerfeld coefficient from the BFSs. However, in general, this cannot be distinguished from impurity effects unless, as shown in [56], it is possible to control the impurity concentration. We note that a supercurrent can be used to experimentally probe the PDW state. In particular, the addition of a supercurrent will change the momentum of the PDW and hence change the size of the BFSs.

VI. CONCLUSIONS

We considered the interplay of \mathcal{PT} translation invariant Kramers' degenerate magnetic order and superconductivity. The absence of \mathcal{P} and \mathcal{T} symmetry leads to an asymmetry in the electronic dispersion relation ($\xi_{\mathbf{k}} \neq \xi_{-\mathbf{k}}$). We develop a general single-band framework to capture the effect of Kramers' degenerate magnetic order on superconductivity. We find that, when the magnetic states belong to a vector representation of the point group, pair density wave states are stabilized. In the absence of such symmetries, superconductivity is generically suppressed. We apply our framework to CeRh_2As_2 , where we explain why superconductivity persists in the presence of Kramers' degenerate magnetic order, as well as to the coexistence of loop current order and superconductivity in the cuprates, where pair density wave superconductivity appears together with Bogoliubov Fermi surfaces.

ACKNOWLEDGMENTS

A.A., H.W., and D.F.A. were supported by the U.S. Department of Energy, Office of Basic Energy Sciences, Division of Materials Sciences and Engineering under Award No. DE-SC0021971. T.S. acknowledges support by the U.S. Department of Energy, Office of Basic Energy Sciences, Division of Materials Sciences and Engineering under Award No. DE-SC0017632. We would like to thank E. Berg, E. Hassinger, S. Khim, S. Kivelson, C. Parsons, T. RoyChowdhury, and M. Weinert for useful discussions.

APPENDIX: DERIVATION OF THE GREEN'S FUNCTIONS

Starting from the single-band Hamiltonian

$$H = \sum_{\mathbf{k}s} \varepsilon_{\mathbf{k}} c_{\mathbf{k}s}^\dagger c_{\mathbf{k}s} + \frac{1}{2} \sum_{\mathbf{k}\mathbf{k}'\alpha\beta\alpha'\beta'} V_{\alpha\beta\alpha'\beta'}(\mathbf{k}, \mathbf{k}') \times c_{\mathbf{k}+\frac{\mathbf{q}}{2},\alpha}^\dagger c_{-\mathbf{k}+\frac{\mathbf{q}}{2},\beta}^\dagger c_{-\mathbf{k}'+\frac{\mathbf{q}}{2},\beta'} c_{\mathbf{k}'+\frac{\mathbf{q}}{2},\alpha'} \quad (\text{A1})$$

within mean-field approximation, we get the mean-field Hamiltonian

$$H = \sum_{\mathbf{k}s} \varepsilon_{\mathbf{k}} c_{\mathbf{k}s}^\dagger c_{\mathbf{k}s} - \frac{1}{2} \sum_{\mathbf{k}\alpha\beta} \Delta_{\alpha\beta}(\mathbf{k}, \mathbf{q}) c_{\mathbf{k}+\frac{\mathbf{q}}{2},\alpha}^\dagger c_{-\mathbf{k}+\frac{\mathbf{q}}{2},\beta}^\dagger - \frac{1}{2} \sum_{\mathbf{k}\alpha\beta} \Delta_{\alpha\beta}^*(\mathbf{k}, \mathbf{q}) c_{-\mathbf{k}+\frac{\mathbf{q}}{2},\beta} c_{\mathbf{k}+\frac{\mathbf{q}}{2},\alpha}, \quad (\text{A2})$$

where we have defined the gap function as

$$\Delta_{\alpha\beta}(\mathbf{k}, \mathbf{q}) \equiv - \sum_{\mathbf{k}'\alpha'\beta'} V_{\alpha\beta\alpha'\beta'}(\mathbf{k}, \mathbf{k}') \langle c_{-\mathbf{k}'+\frac{\mathbf{q}}{2},\beta'} c_{\mathbf{k}'+\frac{\mathbf{q}}{2},\alpha'} \rangle \quad (\text{A3})$$

and then

$$\begin{aligned} \Delta_{\alpha\beta}^*(\mathbf{k}, \mathbf{q}) &= - \sum_{\mathbf{k}'\alpha'\beta'} [V_{\alpha\beta\alpha'\beta'}(\mathbf{k}, \mathbf{k}')]^* \langle c_{-\mathbf{k}'+\frac{\mathbf{q}}{2},\beta'}^\dagger c_{\mathbf{k}'+\frac{\mathbf{q}}{2},\alpha'}^\dagger \rangle^* \\ &= - \sum_{\mathbf{k}'\alpha'\beta'} V_{\alpha'\beta'\alpha\beta}(\mathbf{k}', \mathbf{k}) \langle c_{\mathbf{k}'+\frac{\mathbf{q}}{2},\alpha'}^\dagger c_{-\mathbf{k}'+\frac{\mathbf{q}}{2},\beta'}^\dagger \rangle, \end{aligned} \quad (\text{A4})$$

where $\langle \dots \rangle$ stands for a grand canonical ensemble average. We introduce the finite-temperature Green's function:

$$G_{\alpha\beta}(\mathbf{k}, \mathbf{q}, \tau) \equiv - \langle T_\tau c_{\mathbf{k}+\frac{\mathbf{q}}{2},\alpha}(\tau) c_{\mathbf{k}+\frac{\mathbf{q}}{2},\beta}^\dagger(0) \rangle. \quad (\text{A5})$$

The operator $A(\tau)$ denotes $e^{H\tau/\hbar} A e^{-H\tau/\hbar}$, $A(0)$ is for $\tau = 0$, where H is the Hamiltonian and τ is the ‘‘imaginary time,’’ which is treated as a real quantity. T_τ is the time ordering operator with respect to the imaginary time. Using the Heaviside step function

$$\theta(x) = \begin{cases} 0, & x < 0, \\ 1, & x > 0, \end{cases} \quad (\text{A6})$$

we can express the Green's function as

$$G_{\alpha\beta}(\mathbf{k}, \mathbf{q}, \tau) = -\theta(\tau) \langle c_{\mathbf{k}+\frac{\mathbf{q}}{2}, \alpha}^\dagger(\tau) c_{\mathbf{k}+\frac{\mathbf{q}}{2}, \beta}(0) \rangle + \theta(-\tau) \langle c_{\mathbf{k}+\frac{\mathbf{q}}{2}, \beta}^\dagger(0) c_{\mathbf{k}+\frac{\mathbf{q}}{2}, \alpha}(\tau) \rangle. \quad (\text{A7})$$

Using $\frac{\partial}{\partial \tau} G_{\alpha\beta}(\mathbf{k}, \mathbf{q}, \tau)$, we get the equation of motion for the Green's function:

$$\left(\frac{\partial}{\partial \tau} + \frac{\varepsilon_{\mathbf{k}+\frac{\mathbf{q}}{2}}}{\hbar} \right) G_{\alpha\beta}(\mathbf{k}, \mathbf{q}, \tau) + \frac{1}{\hbar} \sum_{\alpha''} \Delta_{\alpha\alpha''}(\mathbf{k}, \mathbf{q}) \times \langle T_\tau c_{-\mathbf{k}+\frac{\mathbf{q}}{2}, \alpha''}^\dagger(\tau) c_{\mathbf{k}+\frac{\mathbf{q}}{2}, \beta}^\dagger(0) \rangle = -\delta(\tau) \delta_{\alpha\beta}. \quad (\text{A8})$$

We can define the anomalous Green's function:

$$F_{\alpha\beta}^\dagger(\mathbf{k}, \mathbf{q}, \tau) \equiv -\langle T_\tau c_{-\mathbf{k}+\frac{\mathbf{q}}{2}, \alpha}^\dagger(\tau) c_{\mathbf{k}+\frac{\mathbf{q}}{2}, \beta}^\dagger(0) \rangle. \quad (\text{A9})$$

Similarly, using $\frac{\partial}{\partial \tau} F_{\alpha\beta}^\dagger(\mathbf{k}, \mathbf{q}, \tau)$, we get the equation of motion for the anomalous Green's function:

$$\left(\frac{\partial}{\partial \tau} - \frac{\varepsilon_{-\mathbf{k}+\frac{\mathbf{q}}{2}}}{\hbar} \right) F_{\alpha\beta}^\dagger(\mathbf{k}, \mathbf{q}, \tau) - \frac{1}{\hbar} \sum_{\alpha''} \Delta_{\alpha''\alpha}^*(\mathbf{k}, \mathbf{q}) G_{\alpha''\beta}(\mathbf{k}, \mathbf{q}, \tau) = 0. \quad (\text{A10})$$

Transforming the Green's function and the anomalous Green's function from the imaginary-time-momentum space to the frequency-momentum space, we get the Gor'kov equations

$$\left(-i\omega_n + \frac{\varepsilon_{\mathbf{k}+\frac{\mathbf{q}}{2}}}{\hbar} \right) G_{\alpha\beta}(\mathbf{k}, \mathbf{q}, \omega_n) - \frac{1}{\hbar} \sum_{\alpha''} \Delta_{\alpha\alpha''}(\mathbf{k}, \mathbf{q}) F_{\alpha''\beta}^\dagger(\mathbf{k}, \mathbf{q}, \omega_n) = -\delta_{\alpha\beta}, \quad (\text{A11})$$

$$\left(-i\omega_n - \frac{\varepsilon_{-\mathbf{k}+\frac{\mathbf{q}}{2}}}{\hbar} \right) F_{\alpha\beta}^\dagger(\mathbf{k}, \mathbf{q}, \omega_n) - \frac{1}{\hbar} \sum_{\alpha''} \Delta_{\alpha''\alpha}^*(\mathbf{k}, \mathbf{q}) G_{\alpha''\beta}(\mathbf{k}, \mathbf{q}, \omega_n) = 0, \quad (\text{A12})$$

where $\delta_{\alpha\beta}$ is the Kronecker delta. We can define a second anomalous Green's function as

$$F_{\alpha\beta}(\mathbf{k}, \mathbf{q}, \tau) \equiv -\langle T_\tau c_{\mathbf{k}+\frac{\mathbf{q}}{2}, \alpha}(\tau) c_{-\mathbf{k}+\frac{\mathbf{q}}{2}, \beta}(0) \rangle. \quad (\text{A13})$$

Combining the definition of the gap function, the expression of the complex conjugate of the gap function, and the definitions of the anomalous Green's function and the second anomalous Green's function in imaginary-time space and their transformations in frequency space, we can get a relationship:

$$F_{\beta'\alpha'}^\dagger(\mathbf{k}', \mathbf{q}, \omega_n) = [F_{\alpha'\beta'}(\mathbf{k}', \mathbf{q}, \omega_n)]^*. \quad (\text{A14})$$

Then, we can replace the anomalous Green's functions with the second anomalous Green's functions in the Gor'kov

equations to get

$$\left(-i\omega_n + \frac{\varepsilon_{\mathbf{k}+\frac{\mathbf{q}}{2}}}{\hbar} \right) G_{\alpha\beta}(\mathbf{k}, \mathbf{q}, \omega_n) - \frac{1}{\hbar} \sum_{\alpha''} \Delta_{\alpha\alpha''}(\mathbf{k}, \mathbf{q}) [F_{\beta\alpha''}(\mathbf{k}, \mathbf{q}, \omega_n)]^* = -\delta_{\alpha\beta}, \quad (\text{A15})$$

$$\left(-i\omega_n - \frac{\varepsilon_{-\mathbf{k}+\frac{\mathbf{q}}{2}}}{\hbar} \right) [F_{\beta\alpha}(\mathbf{k}, \mathbf{q}, \omega_n)]^* - \frac{1}{\hbar} \sum_{\alpha''} \Delta_{\alpha''\alpha}^*(\mathbf{k}, \mathbf{q}) G_{\alpha''\beta}(\mathbf{k}, \mathbf{q}, \omega_n) = 0. \quad (\text{A16})$$

The Gor'kov equations can be written in a matrix form,

$$\left(-i\hbar\omega_n + \varepsilon_{\mathbf{k}+\frac{\mathbf{q}}{2}} \right) \hat{G} - \hat{\Delta} \hat{F}^\dagger = -\hbar\sigma_0, \quad (\text{A17})$$

$$\left(-i\hbar\omega_n - \varepsilon_{-\mathbf{k}+\frac{\mathbf{q}}{2}} \right) \hat{F}^\dagger - \hat{\Delta}^\dagger \hat{G} = 0, \quad (\text{A18})$$

where $\hat{\Delta}$ is the gap matrix and σ_0 is the identity matrix. Solving this system of matrix equations, we obtain the Green's function and the anomalous Green's function as

$$\hat{G} = -\hbar(\varepsilon_{-\mathbf{k}+\frac{\mathbf{q}}{2}} + i\hbar\omega_n) \times [(\varepsilon_{-\mathbf{k}+\frac{\mathbf{q}}{2}} + i\hbar\omega_n)(\varepsilon_{\mathbf{k}+\frac{\mathbf{q}}{2}} - i\hbar\omega_n)\sigma_0 + \hat{\Delta} \hat{\Delta}^\dagger]^{-1}, \quad (\text{A19})$$

$$\hat{F} = \hbar[(\varepsilon_{-\mathbf{k}+\frac{\mathbf{q}}{2}} - i\hbar\omega_n)(\varepsilon_{\mathbf{k}+\frac{\mathbf{q}}{2}} + i\hbar\omega_n)\sigma_0 + \hat{\Delta} \hat{\Delta}^\dagger]^{-1} \hat{\Delta}. \quad (\text{A20})$$

For singlet pairing, the gap matrix $\hat{\Delta}(\mathbf{k}, \mathbf{q})$ is antisymmetric, which can be characterized by a single even function $\psi(\mathbf{k}, \mathbf{q})$:

$$\hat{\Delta}(\mathbf{k}, \mathbf{q}) = \psi(\mathbf{k}, \mathbf{q}) i\sigma_2 = \begin{bmatrix} 0 & \psi(\mathbf{k}, \mathbf{q}) \\ -\psi(\mathbf{k}, \mathbf{q}) & 0 \end{bmatrix}. \quad (\text{A21})$$

Substituting $\hat{\Delta} \hat{\Delta}^\dagger = |\psi|^2 \sigma_0$ into \hat{G} and \hat{F} , we get the explicit forms of the Green's function and the anomalous Green's function:

$$\hat{G} = -\frac{\hbar(\varepsilon_{-\mathbf{k}+\frac{\mathbf{q}}{2}} + i\hbar\omega_n)\sigma_0}{(\varepsilon_{-\mathbf{k}+\frac{\mathbf{q}}{2}} + i\hbar\omega_n)(\varepsilon_{\mathbf{k}+\frac{\mathbf{q}}{2}} - i\hbar\omega_n) + |\psi(\mathbf{k}, \mathbf{q})|^2}, \quad (\text{A22})$$

$$\hat{F} = \frac{\hbar \hat{\Delta}}{(\varepsilon_{-\mathbf{k}+\frac{\mathbf{q}}{2}} - i\hbar\omega_n)(\varepsilon_{\mathbf{k}+\frac{\mathbf{q}}{2}} + i\hbar\omega_n) + |\psi(\mathbf{k}, \mathbf{q})|^2}. \quad (\text{A23})$$

For triplet pairing, the gap matrix $\hat{\Delta}(\mathbf{k}, \mathbf{q})$ is symmetric, which can be parametrized by an odd vector function $\mathbf{d}(\mathbf{k}, \mathbf{q})$,

$$\hat{\Delta}(\mathbf{k}, \mathbf{q}) = \mathbf{d}(\mathbf{k}, \mathbf{q}) \cdot \boldsymbol{\sigma} i\sigma_2 = \begin{bmatrix} -d_x(\mathbf{k}, \mathbf{q}) + id_y(\mathbf{k}, \mathbf{q}) & d_z(\mathbf{k}, \mathbf{q}) \\ d_z(\mathbf{k}, \mathbf{q}) & d_x(\mathbf{k}, \mathbf{q}) + id_y(\mathbf{k}, \mathbf{q}) \end{bmatrix}, \quad (\text{A24})$$

where the Pauli matrix vector $\boldsymbol{\sigma} = (\sigma_1, \sigma_2, \sigma_3)$. Assuming real $\mathbf{d}(\mathbf{k}, \mathbf{q})$, we have $\hat{\Delta} \hat{\Delta}^\dagger = |\mathbf{d}|^2 \sigma_0$. Substituting this into the solutions for \hat{G} and \hat{F} , we get the explicit forms for the Green's

functions:

$$\hat{G} = -\frac{\hbar(\varepsilon_{-k+\frac{q}{2}} + i\hbar\omega_n)\sigma_0}{(\varepsilon_{-k+\frac{q}{2}} + i\hbar\omega_n)(\varepsilon_{k+\frac{q}{2}} - i\hbar\omega_n) + |\mathbf{d}(\mathbf{k}, \mathbf{q})|^2}, \quad (\text{A25})$$

$$\hat{F} = \frac{\hbar\hat{\Delta}}{(\varepsilon_{-k+\frac{q}{2}} - i\hbar\omega_n)(\varepsilon_{k+\frac{q}{2}} + i\hbar\omega_n) + |\mathbf{d}(\mathbf{k}, \mathbf{q})|^2}. \quad (\text{A26})$$

- [1] S. Khim, J. F. Landaeta, J. Banda, N. Bannor, M. Brando, P. M. R. Brydon, D. Hafner, R. Küchler, R. Cardoso-Gil, U. Stockert, A. P. Mackenzie, D. F. Agterberg, C. Geibel, and E. Hassinger, Field-induced transition within the superconducting state of CeRh₂As₂, *Science* **373**, 1012 (2021).
- [2] E. G. Schertenleib, M. H. Fischer, and M. Sigrist, Unusual H - T phase diagram of CeRh₂As₂: The role of staggered non-centrosymmetry, *Phys. Rev. Res.* **3**, 023179 (2021).
- [3] A. Ptok, K. J. Kapcia, P. T. Jochym, J. Łażewski, A. M. Oleś, and P. Piekarczyk, Electronic and dynamical properties of CeRh₂As₂: Role of Rh₂As₂ layers and expected orbital order, *Phys. Rev. B* **104**, L041109 (2021).
- [4] D. Möckli and A. Ramires, Two scenarios for superconductivity in CeRh₂As₂, *Phys. Rev. Res.* **3**, 023204 (2021).
- [5] A. Skurativska, M. Sigrist, and M. H. Fischer, Spin response and topology of a staggered-Rashba superconductor, *Phys. Rev. Res.* **3**, 033133 (2021).
- [6] K. Nogaki, A. Daido, J. Ishizuka, and Y. Yanase, Topological crystalline superconductivity in locally noncentrosymmetric CeRh₂As₂, *Phys. Rev. Res.* **3**, L032071 (2021).
- [7] D. C. Cavanagh, T. Shishidou, M. Weinert, P. M. R. Brydon, and D. F. Agterberg, Nonsymmorphic symmetry and field-driven odd-parity pairing in CeRh₂As₂, *Phys. Rev. B* **105**, L020505 (2022).
- [8] J. F. Landaeta, P. Khanenko, D. C. Cavanagh, C. Geibel, S. Khim, S. Mishra, I. Sheikin, P. M. R. Brydon, D. F. Agterberg, M. Brando, and E. Hassinger, Field-angle dependence reveals odd-parity superconductivity in CeRh₂As₂, *Phys. Rev. X* **12**, 031001 (2022).
- [9] K. Nogaki and Y. Yanase, Even-odd parity transition in strongly correlated locally noncentrosymmetric superconductors: Application to CeRh₂As₂, *Phys. Rev. B* **106**, L100504 (2022).
- [10] D. Möckli and A. Ramires, Superconductivity in disordered locally noncentrosymmetric materials: An application to CeRh₂As₂, *Phys. Rev. B* **104**, 134517 (2021).
- [11] T. Hazra and P. Coleman, Triplet pairing mechanisms from Hund's-Kondo models: Applications to UTe₃ and CeRh₂As₂, *Phys. Rev. Lett.* **130**, 136002 (2023).
- [12] S. Mishra, Y. Liu, E. D. Bauer, F. Ronning, and S. M. Thomas, Anisotropic magnetotransport properties of the heavy-fermion superconductor CeRh₂As₂, *Phys. Rev. B* **106**, L140502 (2022).
- [13] S.-I. Kimura, J. Sichelschmidt, and S. Khim, Optical study of the electronic structure of locally noncentrosymmetric CeRh₂As₂, *Phys. Rev. B* **104**, 245116 (2021).
- [14] K. Machida, Violation of Pauli-Clogston limit in the heavy-fermion superconductor CeRh₂As₂: Duality of itinerant and localized 4f electrons, *Phys. Rev. B* **106**, 184509 (2022).
- [15] K. Semeniuk, D. Hafner, P. Khanenko, T. Lühmann, J. Banda, J. F. Landaeta, C. Geibel, S. Khim, E. Hassinger, and M. Brando, Superconductivity versus quadrupole density wave in CeRh₂As₂, [arXiv:2301.09151](https://arxiv.org/abs/2301.09151).
- [16] S. Onishi, U. Stockert, S. Khim, J. Banda, M. Brando, and E. Hassinger, Low-temperature thermal conductivity of the two-phase superconductor CeRh₂As₂, *Front. Electron. Mater.* **2**, 880579 (2022).
- [17] M. Kibune, S. Kitagawa, K. Kinjo, S. Ogata, M. Manago, T. Taniguchi, K. Ishida, M. Brando, E. Hassinger, H. Rosner *et al.*, Observation of antiferromagnetic order as odd-parity multipoles inside the superconducting phase in CeRh₂As₂, *Phys. Rev. Lett.* **128**, 057002 (2022).
- [18] S. Kitagawa, M. Kibune, K. Kinjo, M. Manago, T. Taniguchi, K. Ishida, M. Brando, E. Hassinger, C. Geibel, and S. Khim, Two-dimensional XY-type magnetic properties of locally non-centrosymmetric superconductor CeRh₂As₂, *J. Phys. Soc. Jpn.* **91**, 043702 (2022).
- [19] S. Sumita and Y. Yanase, Superconductivity in magnetic multipole states, *Phys. Rev. B* **93**, 224507 (2016).
- [20] S. Hayami, M. Yatsushiro, Y. Yanagi, and H. Kusunose, Classification of atomic-scale multipoles under crystallographic point groups and application to linear response tensors, *Phys. Rev. B* **98**, 165110 (2018).
- [21] H. Wu, A. Amin, Y. Yu, and D. F. Agterberg, Nematic Bogoliubov Fermi surfaces from magnetic toroidal order in FeSe_{1-x}S_x, [arXiv:2306.11200](https://arxiv.org/abs/2306.11200).
- [22] S. Sumita, T. Nomoto, and Y. Yanase, Multipole superconductivity in nonsymmorphic Sr₂IrO₄, *Phys. Rev. Lett.* **119**, 027001 (2017).
- [23] E. Berg, C.-C. Chen, and S. A. Kivelson, Stability of nodal quasiparticles in superconductors with coexisting orders, *Phys. Rev. Lett.* **100**, 027003 (2008).
- [24] A. Allais and T. Senthil, Loop current order and d-wave superconductivity: Some observable consequences, *Phys. Rev. B* **86**, 045118 (2012).
- [25] L. Wang and O. Vafek, Quantum oscillations of the specific heat in d-wave superconductors with loop current order, *Phys. Rev. B* **88**, 024506 (2013).
- [26] J. W. Serene and D. Rainer, The quasiclassical approach to superfluid ³He, *Phys. Rep.* **101**, 221 (1983).
- [27] T. Nagashima, T. Hashimoto, S. Najafzadeh, S.-i. Ouchi, T. Suzuki, A. Fukushima, S. Kasahara, K. Matsuura, M. Qiu, Y. Mizukami, K. Hashimoto, Y. Matsuda, T. Shibauchi, S. Shin, and K. Okazaki, Discovery of nematic Bogoliubov Fermi surface in an iron-chalcogenide superconductor, Research Square report (2022), doi: [10.21203/rs.3.rs-2224728/v1](https://doi.org/10.21203/rs.3.rs-2224728/v1).
- [28] O. Fedchenko, L. Šmejkal, M. Kallmayer, Y. Lytvynenko, K. Medjanik, S. Babenkov, D. Vasilyev, M. Klauui, J. Demsar, G. Schönhense *et al.*, Direct observation of antiferromagnetic parity violation in the electronic structure of Mn₂Au, *J. Phys.: Condens. Matter* **34**, 425501 (2022).
- [29] L. Šmejkal, J. Železný, J. Sinova, and T. Jungwirth, Electric control of Dirac quasiparticles by spin-orbit torque in an antiferromagnet, *Phys. Rev. Lett.* **118**, 106402 (2017).
- [30] A. Urru, J.-R. Soh, N. Qureshi, A. Stunault, B. Roessli, H. M. Rønnow, and N. A. Spaldin, Neutron scattering from local magnetoelectric multipoles: A combined theoretical,

- computational, and experimental perspective, *Phys. Rev. Res.* **5**, 033147 (2023).
- [31] S. Bhowal and N. A. Spaldin, Revealing hidden magnetoelectric multipoles using Compton scattering, *Phys. Rev. Res.* **3**, 033185 (2021).
- [32] N. A. Spaldin and R. Ramesh, Advances in magnetoelectric multiferroics, *Nat. Mater.* **18**, 203 (2019).
- [33] M. Yatsushiro, R. Oiwa, H. Kusunose, and S. Hayami, Analysis of model-parameter dependences on the second-order nonlinear conductivity in \mathcal{PT} -symmetric collinear antiferromagnetic metals with magnetic toroidal moment on zigzag chains, *Phys. Rev. B* **105**, 155157 (2022).
- [34] S. Hayami, M. Yatsushiro, and H. Kusunose, Nonlinear spin Hall effect in \mathcal{PT} -symmetric collinear magnets, *Phys. Rev. B* **106**, 024405 (2022).
- [35] C. M. Varma, Non-Fermi-liquid states and pairing instability of a general model of copper oxide metals, *Phys. Rev. B* **55**, 14554 (1997).
- [36] C. M. Varma, Pseudogap phase and the quantum-critical point in copper-oxide metals, *Phys. Rev. Lett.* **83**, 3538 (1999).
- [37] M. E. Simon and C. M. Varma, Detection and implications of a time-reversal breaking state in underdoped cuprates, *Phys. Rev. Lett.* **89**, 247003 (2002).
- [38] C. M. Varma, Theory of the pseudogap state of the cuprates, *Phys. Rev. B* **73**, 155113 (2006).
- [39] M. Sigrist and K. Ueda, Phenomenological theory of unconventional superconductivity, *Rev. Mod. Phys.* **63**, 239 (1991).
- [40] L. P. Gor'kov and E. I. Rashba, Superconducting 2D system with lifted spin degeneracy: Mixed singlet-triplet state, *Phys. Rev. Lett.* **87**, 037004 (2001).
- [41] D. F. Agterberg, J. C. S. Davis, S. D. Edkins, E. Fradkin, D. J. V. Harlingen, S. A. Kivelson, P. A. Lee, L. Radzihovsky, J. M. Tranquada, and Y. Wang, The physics of pair-density waves: Cuprate superconductors and beyond, *Annu. Rev. Condens. Matter Phys.* **11**, 231 (2020).
- [42] N. F. Q. Yuan and L. Fu, Supercurrent diode effect and finite-momentum superconductors, *Proc. Natl. Acad. Sci. USA* **119**, e2119548119 (2022).
- [43] J. J. He, Y. Tanaka, and N. Nagaosa, A phenomenological theory of superconductor diodes, *New J. Phys.* **24**, 053014 (2022).
- [44] A. Daido, Y. Ikeda, and Y. Yanase, Intrinsic superconducting diode effect, *Phys. Rev. Lett.* **128**, 037001 (2022).
- [45] B. Pal, A. Chakraborty, P. K. Sivakumar, M. Davydova, A. K. Gopi, A. K. Pandeya, J. A. Krieger, Y. Zhang, M. Date, S. Ju *et al.*, Josephson diode effect from Cooper pair momentum in a topological semimetal, *Nat. Phys.* **18**, 1228 (2022).
- [46] D. F. Agterberg, P. M. R. Brydon, and C. Timm, Bogoliubov Fermi surfaces in superconductors with broken time-reversal symmetry, *Phys. Rev. Lett.* **118**, 127001 (2017).
- [47] P. M. R. Brydon, D. F. Agterberg, H. Menke, and C. Timm, Bogoliubov Fermi surfaces: General theory, magnetic order, and topology, *Phys. Rev. B* **98**, 224509 (2018).
- [48] J. M. Link and I. F. Herbut, Bogoliubov-Fermi surfaces in non-centrosymmetric multicomponent superconductors, *Phys. Rev. Lett.* **125**, 237004 (2020).
- [49] C. Timm, A. P. Schnyder, D. F. Agterberg, and P. M. R. Brydon, Inflated nodes and surface states in superconducting half-Heusler compounds, *Phys. Rev. B* **96**, 094526 (2017).
- [50] D. Hafner, P. Khanenko, E.-O. Eljaouhari, R. Kuchler, J. Banda, N. Bannor, T. Lühmann, J. F. Landaeta, S. Mishra, I. Sheikin, E. Hassinger, S. Khim, C. Geibel, G. Zwicknagl, and M. Brando, Possible quadrupole density wave in the superconducting Kondo lattice CeRh₂As₂, *Phys. Rev. X* **12**, 011023 (2022).
- [51] T. Shishidou (unpublished).
- [52] H. G. Suh, Y. Yu, T. Shishidou, M. Weinert, P. M. R. Brydon, and D. F. Agterberg, Superconductivity of anomalous pseudospin in nonsymmorphic materials, *Phys. Rev. Res.* **5**, 033204 (2023).
- [53] X. Chen, L. Wang, J. Ishizuka, K. Nogaki, Y. Cheng, F. Yang, R. Zhang, Z. Chen, F. Zhu, Y. Yanase *et al.*, Coexistence of near-EF flat band and van Hove singularity in a two-phase superconductor, [arXiv:2309.05895](https://arxiv.org/abs/2309.05895).
- [54] Y. Wu, Y. Zhang, S. Ju, Y. Hu, G. Yang, H. Zheng, Y. Huang, Y. Zhang, H. Zhang, B. Song *et al.*, Quasi-two-dimensional Fermi surface and heavy quasiparticles in CeRh₂As₂, [arXiv:2309.06732](https://arxiv.org/abs/2309.06732).
- [55] S. A. Kivelson and C. M. Varma, Fermi pockets in a d-wave superconductor with coexisting loop-current order, [arXiv:1208.6498](https://arxiv.org/abs/1208.6498).
- [56] H. Oh, D. F. Agterberg, and E.-G. Moon, Using disorder to identify Bogoliubov Fermi-surface states, *Phys. Rev. Lett.* **127**, 257002 (2021).